



# Vibration analysis based on time-frequency analysis with a digital filter: Application to nonlinear system identification

Yoshiaki ITOH<sup>1</sup>; Taku IMAZU<sup>2</sup>; Hiroki NAKAMURA<sup>3</sup>; Toru YAMAZAKI<sup>4</sup>

<sup>1</sup> Kanagawa Industrial Technology Research Center, Japan

<sup>2</sup> Graduate Student, Kanagawa University, Japan

<sup>3,4</sup> Department of Mechanical Engineering, Kanagawa University, Japan

## ABSTRACT

The main purpose of this study is to model and identify the mechanical systems from their output signals of vibrations. The time-frequency analysis method based on infinite impulse response (IIR) digital filter technology is applied to identify nonlinear vibrations. In our previous research, the advantage of the time-frequency analysis procedure over FFT analysis was shown. Here, as a typical weakly nonlinear system, we discuss the time-frequency analysis of the Duffing equation. The time-frequency analysis results and the appropriate analytical solution are compared at steady state. Then, the numerical solutions of the Duffing equation for transient and non-stationary states, including passage through resonance phenomena, are examined with the use of the time-frequency analysis. Furthermore, the basic concept for an application to nonlinear system identification by the time-frequency analysis is discussed.

Keywords: Time-Frequency Analysis, Nonlinear Vibration, Modeling  
I-INCE Classification of Subjects Number(s): 74.3

## 1. INTRODUCTION

Vibrations of any mechanical systems are unavoidable whenever they are running. The more the systems are reduced in size and weight, the larger the effect of nonlinear vibration and the greater the occurrence of nonlinear resonances becomes. These nonlinear vibrations are mainly caused by geometrical and material nonlinearities (1). Nonlinearities may cause the occurrence of unexpected vibrations. In general, vibrations shorten the life of equipment, degrade quality, cause serious accidents, inflict damage, and produce other negative outcomes. For these reasons, measurements of mechanical vibrations are taken as part of vibration diagnosis systems during machine maintenance and daily operations (2). In particular, transient and time-varying non-stationary vibrations as well as steady-state vibrations must be considered before the practical design of any mechanical systems and in machine diagnostics.

Fast Fourier Transform (FFT) is a well-known technique for analyzing periodic steady-state or quasi-steady vibrations with slowly varying frequencies. In contrast, Short Time Fourier Transform (STFT) and Wavelet Transform (WT) are suitable for analyzing transient or non-stationary phenomena. STFT is the most applicable method for studying transient signals. The basic idea of STFT begins with FFT and breaks up the signal into small time segments; each time segment is then analyzed by FFT to ascertain the component frequencies (3, 4). The totality of such spectra indicates

---

<sup>1</sup> itoh@kanagawa-iri.jp

<sup>2</sup> r201370081pe@kanagawa-u.ac.jp

<sup>3</sup> hiroki-nak@kanagawa-u.ac.jp

<sup>4</sup> toru@kanagawa-u.ac.jp

how the spectrum varies over time. WT is a mathematical technique for the analysis of signals whose frequency varies over time (5). WT is well suited for analyzing signal traits such as overall trend, breakdown points, and discontinuities.

Several properties of transient and non-stationary mechanical vibrations have been studied, such as the passage of rotor vibrations through resonance (6), impact and collision phenomena (7), and corrugation between a brake pad and disc (8). Impact phenomena have also been studied by considering the energy transfer among structure membranes using statistical energy analysis (9, 10).

In contrast, we have proposed an analytical method based on infinite impulse response (IIR) digital filter technology (11) to analyze the transient and non-stationary vibrations as well as steady-state vibrations. The method is called “time-frequency analysis”. In a previous study (12), we introduced the time frequency analysis procedure and the algorithm that implements it. The results of our analysis for steady-state vibration were verified as equivalent to those from FFT analyses. Transient and non-stationary vibrations could also be analyzed with comparable ease using this method. The use of inverse analysis to construct the vibration model was also discussed from the viewpoint of identification (13). Moreover, the time-frequency analysis method has the advantage that the vibration can be analyzed more easily than with STFT and WT. This is because STFT requires complex analysis so that higher skill and understanding is necessary; in WT we must also choose a wavelet prototype function, called the mother wavelet.

As a practical application of time-frequency analysis, we modeled the vibration transmission between a violin body and its bridge in order to derive some useful information on the reduction of mechanical vibrations in contact conditions (14, 15).

In this paper, we apply the time-frequency analysis to the identification of nonlinear vibrations. Our previous research (12) indicated that the advantage of the time-frequency analysis procedure over FFT analysis lies in the capability for transient and non-stationary vibration analyses. We discuss the time-frequency analysis of the Duffing equation, as a typical weakly nonlinear system (16). Thus, comparison between the time-frequency analysis result and the appropriate analytical solution is made at steady state. The time-frequency analysis of the Duffing equation for transient and non-stationary responses, representing passage through resonance phenomena, is examined. Furthermore, the basic concept for an application to nonlinear system identification by the time-frequency analysis is discussed.

## 2. TIME-FREQUENCY ANALYSIS WITH A DIGITAL FILTER

Time-frequency analysis with a digital filter and the general ideas associated with it are introduced in this section.

Figure 1 shows the digital filter system for processing a continuous time signal  $x(t)$  into a discrete time-frequency analysis result  $X(n\Delta T, f)$ . The basic characteristic of the method lies in parallel processing by adapting multiple band-pass filters, each of which is based on IIR digital filter technology (11). Thus, we regard the band-pass digital filter as a tool for understanding both the time and frequency domains simultaneously.

In our previous study (12), the time-frequency analysis results were shown to have the same qualitative properties as FFT results for steady-state vibrations. The advantage of using the method is that not only transient responses, composed of free-damped-oscillation terms and forced-excitation terms, but also non-stationary responses, having time-dependent frequencies and amplitudes, can be analyzed with ease. In contrast analytical procedures for these responses are difficult, and require extensive mathematical study.

The schematic procedure for the time-frequency analysis is detailed in (12, 13). Here, only an outline is given. The fundamental technology applies both analogue and digital filter technologies, primarily (i) band-pass filter design, (ii) forward and reverse time-domain digital filter processing, and (iii) calculation of the instantaneous envelope of filtered output signals. It is obvious that the time-frequency analysis cannot be realized by these components separately. The system is composed of multiple narrow-band band-pass filters in order to understand the general properties of the time-frequency distribution in which each bandwidth differs slightly from the others.

As shown in Figure 1, the digital filter system is composed of  $K$  narrow-band digital band-pass filter processes  $BPF_k$  ( $k = 1, 2, \dots, K$ ) with transform functions  $H_k(z)$  ( $k = 1, 2, \dots, K$ ). The transform function  $H_k(z)$  of each band-pass filter is given by

$$H_k(z) = \frac{b_0 + b_1z^{-1} + b_2z^{-2} + \dots + b_Mz^{-M}}{1 + a_1z^{-1} + a_2z^{-2} + \dots + a_Nz^{-N}} \quad (1)$$

In Eq. (1),  $a_i (i=1,2,\dots,N)$  and  $b_j (j=1,2,\dots,M)$  are constants determining the transform function of each band-pass filter. A noteworthy characteristic of our digital filter system is that multiple band-pass filters, each with slightly different pass-bands, are implemented in order to recognize the time-frequency distribution of the output signal.

First of all, the continuous time function  $x(t)$  is converted to a discrete time sequence  $x(n\Delta T)$  ( $n = 1, 2, \dots$ ) with sampling period  $\Delta T$ . The discrete time sequence  $x(n\Delta T)$  is transferred through the IIR digital filter. Consequently, the discrete time-frequency analysis result  $X(n\Delta T, f)$ , a family of functions of time and frequency, is obtained. As a result, we can obtain the time-frequency analysis distributions  $X(t, f)$  as functions of time and frequency domains.

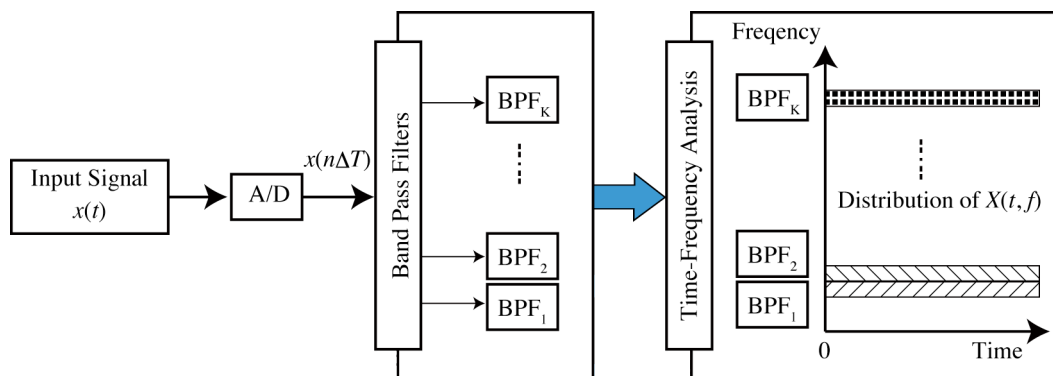


Figure 1 – Digital filter system for time-frequency analysis

### 3. TIME-FREQUENCY ANALYSIS FOR NONLINEAR PHENOMENA

A property of time-frequency analysis is that vibrations can be analyzed using the output signal itself (12). Thus, we can understand the behavior of a system without considering whether the system is in steady state or not. Below, the primary and secondary resonances of the Duffing equation (16) are discussed as representative nonlinear phenomena.

#### 3.1. Duffing Equation

The Duffing equation, given by

$$\ddot{u} + \omega^2 u = -2\hat{\mu}\dot{u} - \hat{\alpha}u^3 + \hat{\kappa} \cos \Omega t, \quad (2)$$

is used to examine the nonlinear effects of any mechanical vibrations. Here, the damping coefficient  $\hat{\mu}$  is positive and the coefficient of the nonlinear term  $\hat{\alpha}$  can be either a positive or a negative constant. For simplicity the system has constant parameters.

Since the Duffing equation contains a cubic nonlinearity, the system exhibits frequency hysteresis behavior, called jump phenomena, and secondary resonances. Most discussion has been focused on obtaining steady-state solutions, derived from analytical expressions and numerical calculations. On the other hand, both transient and non-stationary vibrations are difficult to analyze systematically. In particular, when the frequency of the excitation is time-dependent, the response near the resonance conditions experiences passage through resonance. Since analytical expressions for non-stationary responses are limited to the case where the excitation frequency is slowly varied, *i.e.*, quasi-steady responses, it is difficult to analyze mechanical vibrations at machine startup or shutdown.

#### 3.2. Primary Resonance of the Duffing Equation

The primary resonance of the Duffing equation occurs when  $\Omega \approx \omega$ . Here, the output signals  $\hat{u}(t)$  given by Eq. (2) are analyzed with the use of the time-frequency analysis procedure.

Figure 2 shows the time history of Eq. (2) at  $\Omega = \omega$ , and its time-frequency analysis distribution. Here,  $\omega = 1$ ,  $\hat{\mu} = 0.07$ ,  $\hat{\alpha} = 0.07$  and  $\hat{\kappa} = 0.03$ . The vibration is increased gradually compared to the linear excitation and exhibits some beating behaviors in the process of the transient region. After about  $t \approx 600$  the vibration reaches a steady state. At  $\Omega = \omega$ , the amplitude of the response for the

nonlinear case ( $\hat{\alpha} \neq 0$ ) is smaller than that for linear case ( $\hat{\alpha} = 0$ ).

Figure 2 (b) shows the time-frequency analysis distribution  $U(t, f)$  of  $u(t)$  illustrated by color contour mapping, where the horizontal axis is time  $t$  and the vertical axis is the nominal pass-band center frequency of each band-pass filter  $BPF_k$  ( $k = 1, 2, \dots, K$ ). Here, discrete-time signals  $u(n\Delta T)$  of the continuous-time signal  $u(t)$  are sampled with non-dimensional period  $\Delta T = 0.01$ . In the following, the time-frequency analysis is performed under the conditions that the number of band-pass filters  $K=2048$  and the non-dimensional maximum analysis frequency is equal to 1.

It can be seen from Figure 2 (b) that in the resonant condition,  $u(t)$  is excited only with frequency  $\Omega$ . As mentioned in (12) concerning the linear analyses, the transient phenomena from the start of excitation until the steady-state condition can be explained with the use of the time-frequency analysis. Moreover, the peak amplitude excited with frequency  $\Omega$  corresponds to the excitation frequency found in FFT.

If the excitation frequency  $\Omega$  is time-dependent, then the response becomes non-stationary. Generally, non-stationary vibrations during passage through resonance are observed for time-dependent angular speeds. For safety in rotating machines (1), the rotor must pass the resonance point at startup and shutdown when the amplitude is small.

Figures 3 and 4 show the time histories and their time-frequency analysis distributions for non-stationary responses. Here, we introduce the effect of varying the rate  $r$  of the excitation frequency  $\Omega$ , defined in Eq. (9). Moreover,  $\sigma$  is the detuning parameter defined in Eq. (4). Both parameters are discussed in detail in Section 4.

As shown in Figure 3 (a) for increasing excitation frequency  $r > 0$ , the vibration rapidly increases when the excitation frequency enters the resonance region. After the peak amplitude is passed at  $t \approx 21000$ ,  $\sigma \approx 6.5$ , the vibration decays drastically. As shown in Figure 3 (b), we can observe the details of the vibration such as the jump phenomena at passage through resonance.

On the other hand, as shown in Figure 4 (a) for decreasing excitation frequency  $r < 0$ , the vibration gradually increases as time elapses. At  $t \approx 12000$ ,  $\sigma \approx 3$ , the vibration suddenly increases and reaches a peak. After this, the amplitude gradually decays even though the excitation frequency  $\Omega$  is approaching the natural frequency  $\omega$ .

It is obvious from the time-frequency analysis distributions that the existence of the nonlinearity can be easily examined by increasing and decreasing  $\sigma$  throughout the passage through resonance. If the vibration is widely excited for increasing  $\sigma$ , then the system has the properties of a hard spring, and vice versa. Moreover, if beating phenomena are observed several times, then the rate  $r$  of increase or decrease of the frequency of the excitation is relatively fast. Therefore, the peak amplitude at resonance is small compared to the quasi-steady response of the system. For a non-stationary response, the excitation frequency varies as time elapses, and the free damped vibration is observed after frequency  $\omega$ . If the excitation frequency passes the natural frequency, then the free damped vibration excited with frequency  $\omega$  decays.

In practical mechanical systems, it is necessary to clarify system properties such as the natural frequency, modes, and steady-state response to prevent serious accidents. This leads to the development of vibration diagnosis systems, crack detection systems, and on the like (2).

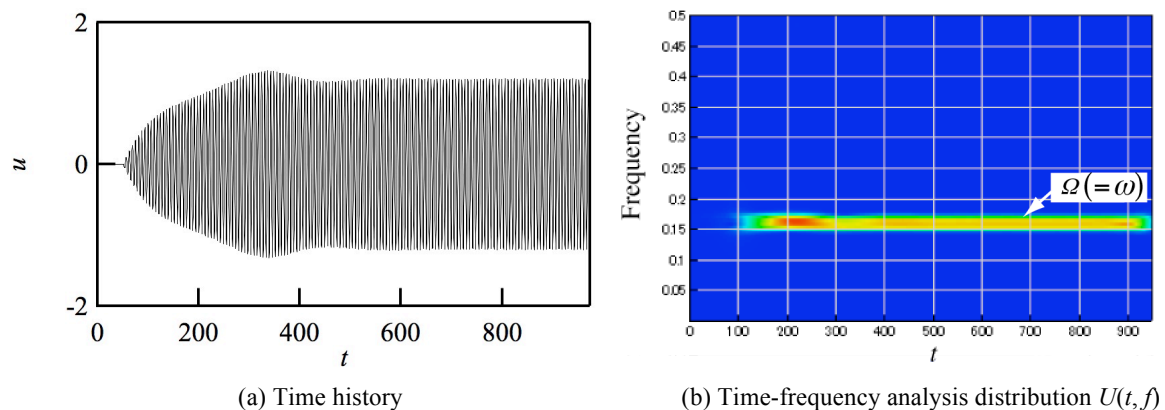


Figure 2 – Time-frequency analysis of the primary resonance of the Duffing equation

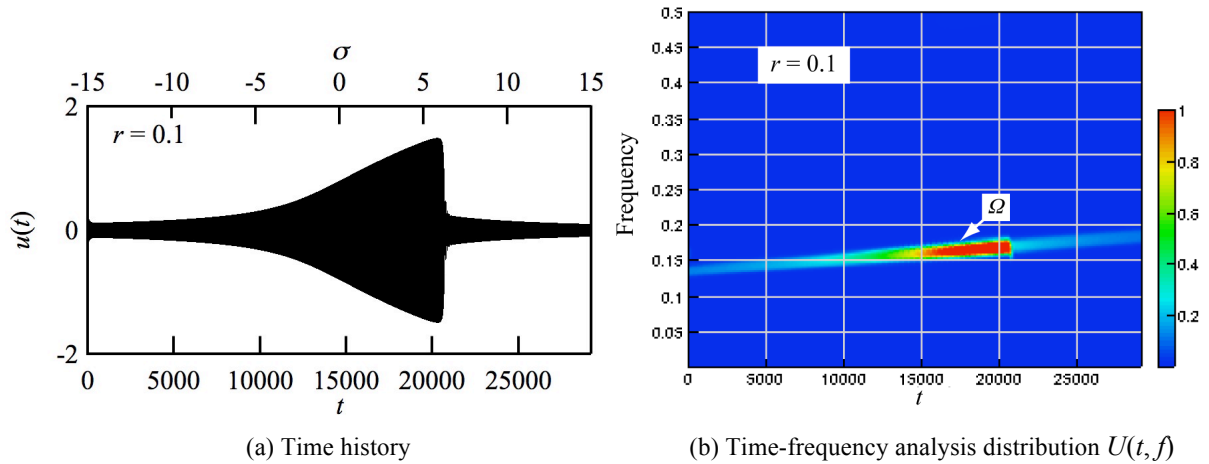


Figure 3 – Time-frequency analysis for a non-stationary primary resonance,  $r = 0.1$

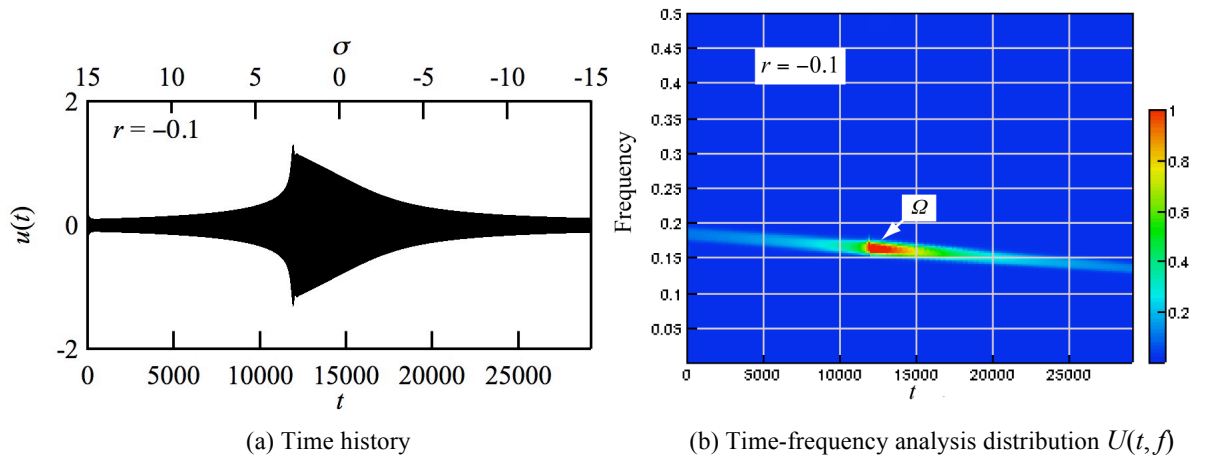


Figure 4 – Time-frequency analysis for a non-stationary primary resonance,  $r = -0.1$

### 3.3. Secondary Resonance of the Duffing Equation

The secondary resonance of the Duffing equation occurs through the effect of the nonlinear term  $\hat{\alpha}u^3$  when  $\Omega \approx \omega/3$ ,  $\Omega \approx 3\omega$ , and so on. In the secondary resonance condition, the steady-state response consists not only of the particular solution excited with  $\Omega$  but also of the solutions excited with natural frequency  $\omega$  equal to  $3\Omega$  or  $\Omega/3$ .

In the following, the superharmonic resonance of order 3 is discussed as a representative secondary resonance (16). The output signals  $u(t)$  of the Duffing equation given by Eq. (2) at  $\Omega = \omega/3$  are analyzed using the time-frequency analysis procedure. Figure 5 shows the time history and its time-frequency analysis distribution. Here,  $\omega = 1$ ,  $\hat{\mu} = 0.01$ ,  $\hat{\alpha} = 0.07$  and  $\hat{\kappa} = 3$ . In the transient region, the vibration suddenly increases and exhibits beating behavior. After about  $t \approx 400$  the vibration reaches a steady state. As shown in Figure 5 (b), at steady state, the vibration is excited with not only the excitation frequency  $\Omega$  but also  $3\Omega$  corresponding to its natural frequency  $\omega$ , due to the effect of the nonlinear term  $\hat{\alpha}u^3$ .

It is very difficult to extract the existence of the vibration excited with  $\Omega$  ( $=\omega/3$ ) from the result shown in Figure 5 (a). As shown in Figure 5 (b), the excitation frequency from startup to the steady state vibration can be easily shown by the use of the time-frequency analysis. On the other hand, if  $\hat{\alpha} = 0$ , then the vibration excited with  $\Omega$  ( $=3\omega$ ) decays and becomes zero at steady state.

Figures 6 and 7 show the time histories and their time-frequency analysis distributions for non-stationary responses. As shown in Figure 6, for increasing excitation frequency  $r > 0$ , the vibration increases and becomes large when the excitation frequency enters the resonance region. The free-vibration term is also excited with  $3\Omega$  ( $=\omega$ ) throughout the secondary resonance region due to the existence of the nonlinear term. After the peak amplitude is passed at  $t \approx 19000$ ,  $\sigma \approx 10$ , the

vibration decays drastically.

On the other hand, as shown in Figure 7 (a) for decreasing excitation frequency  $r < 0$ , the vibration gradually increases as time elapses. At  $t \approx 12000$ ,  $\sigma \approx 5$ , the vibration encounters its peak. After this, the amplitude gradually decays even though the excitation frequency  $\Omega$  is approaching the secondary resonance region. As shown in Figure 7 (b), the free-vibration term is also excited with  $3\Omega (= \omega)$  throughout the secondary resonance region due to the existence of the nonlinear term.

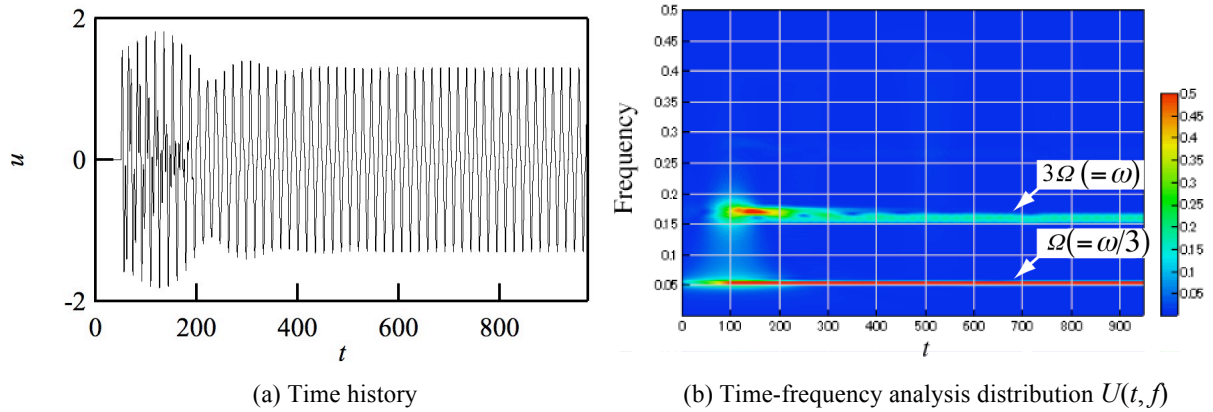


Figure 5 – Time-frequency analysis of the secondary resonance of the Duffing equation

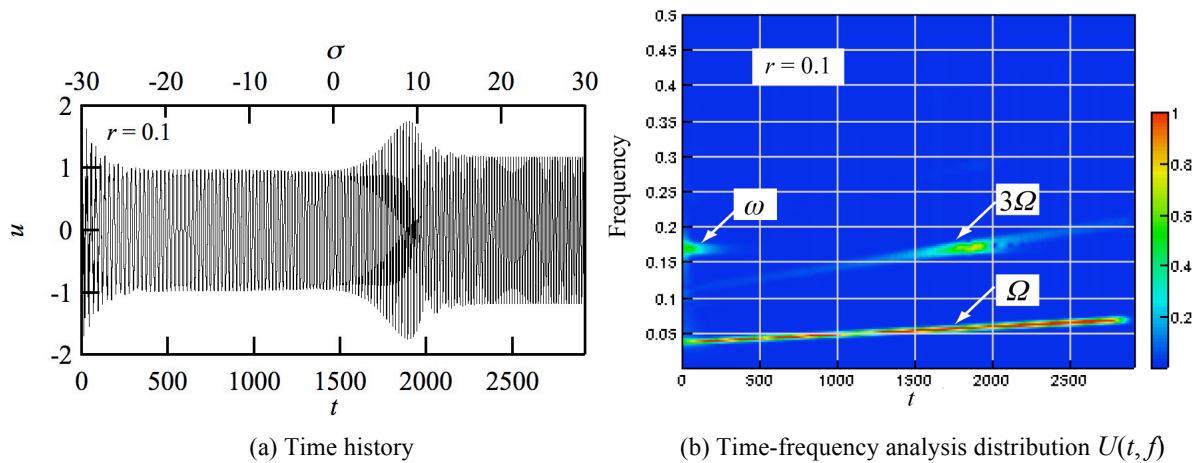


Figure 6 – Time-frequency analysis for a non-stationary secondary resonance,  $r = 0.1$

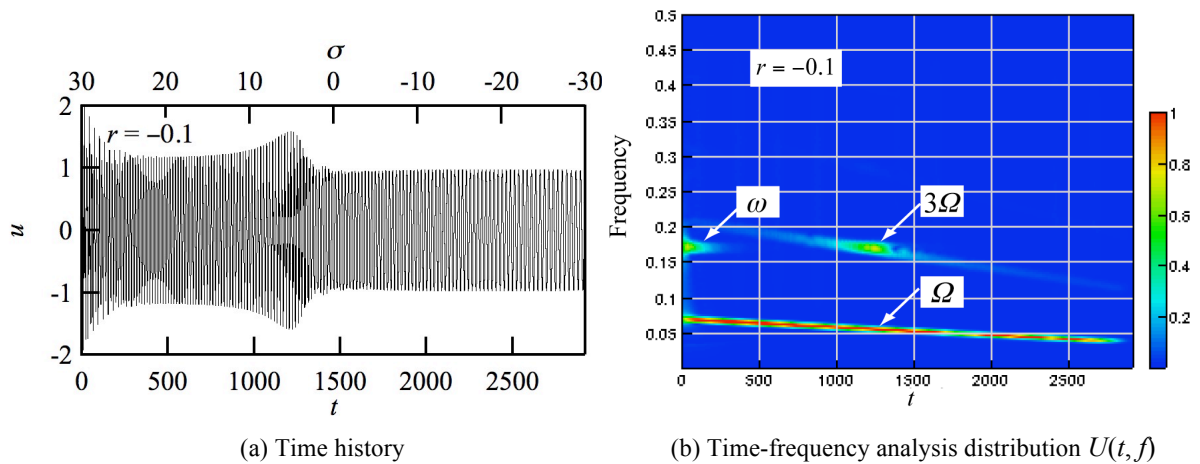


Figure 7 – Time-frequency analysis for a non-stationary secondary resonance,  $r = -0.1$

## 4. DISCUSSION ON MODELING OF NONLINEAR SYSTEMS

### 4.1. Comparison between Time-Frequency Analysis and Approximate Analysis

Approximate expressions for the Duffing equation with external harmonic excitation are considered in order to evaluate the time-frequency analysis results. The method of multiple scales, a well-known perturbation method in nonlinear analyses (16), is applied to derive an approximate analytical solution for a weakly nonlinear system.

#### (1) Primary Resonance

We consider the primary resonance of the Duffing equation. Here, we order  $\hat{\mu} = \varepsilon\mu$ ,  $\hat{\alpha} = \varepsilon\alpha$ , respectively, by introducing a small parameter  $\varepsilon$ . Moreover, to obtain a uniformly valid approximate solution of Eq. (2), we order the excitation  $\kappa = \varepsilon\hat{\kappa}$  so that the damping and the nonlinearity will appear in the same order. Thus, we consider the ordered nonlinear system given by

$$\ddot{u} + \omega^2 u = -2\varepsilon\mu\dot{u} - \varepsilon\alpha u^3 + \varepsilon\kappa \cos \Omega t, \quad (3)$$

where the external excitation frequency  $\Omega$  is expressed by introducing the detuning parameter  $\sigma$  as

$$\Omega = \omega + \varepsilon\sigma t. \quad (4)$$

The procedure to obtain an approximate analytical solution of Eq. (3) is detailed in (16). The first order approximate solution is assumed to be

$$u(t) = a(t) \cos(\Omega t - \gamma) + O(\varepsilon), \quad (5)$$

where the amplitude  $a$  and phase difference  $\gamma$  are determined by the differential equations

$$\frac{da}{dt} = \varepsilon \left( -\mu a + \frac{\kappa}{2\omega} \sin \gamma \right) \quad \text{and} \quad (6)$$

$$a \frac{d\gamma}{dt} = \varepsilon \left( \sigma a - \frac{3\alpha}{8\omega} a^3 + \frac{\kappa}{2\omega} \cos \gamma \right). \quad (7)$$

To determine the character of the solutions the singular points, found by setting  $(da/dt) = (d\gamma/dt) = 0$ , can be obtained:

$$\left[ \mu^2 + \left( \sigma - \frac{3\alpha}{8\omega} a^2 \right)^2 \right] a^2 = \frac{\kappa^2}{4\omega^2}. \quad (8)$$

Equation (8) is an implicit equation for the amplitude of the response  $a$  as a function of the detuning parameter  $\sigma$  and the amplitude of the excitation  $\kappa$ . It can be seen that the peak amplitude  $a_p$  is given by  $\kappa/(2\omega\mu)$ , even though the value of  $\alpha$  may change.

In the same way, a non-stationary solution for a slowly varying excitation can be obtained by letting

$$\sigma(\varepsilon t) = \sigma_0 + r\varepsilon t. \quad (9)$$

Here,  $\sigma_0$  and  $r$  are constants;  $r$  corresponds to the rate of increase or decrease of the excitation frequency.

#### (2) Secondary Resonance

Superharmonic resonance may occur when  $\Omega \approx \omega/3$ . In the following, we explain the derivation of the approximate solution at the superharmonic resonance, examined with the use of the time-frequency analysis in Section 3.3. To explain this, we order the excitation  $\kappa = \hat{\kappa}$ , so that both the hard excitation term, excited with frequency  $\Omega$ , and the free-vibration secondary resonance term, excited with frequency  $3\Omega (\approx \omega)$ , will appear in the same order. Thus, the ordered nonlinear system is given by

$$\ddot{u} + \omega^2 u = -2\varepsilon\mu\dot{u} - \varepsilon\alpha u^3 + \kappa \cos \Omega t, \quad (10)$$

where the external excitation frequency  $\Omega$  is expressed by introducing the detuning parameter  $\sigma$  as

$$3\Omega = \omega + \varepsilon\sigma t. \quad (11)$$

The first order approximate solution is assumed to be

$$u(t) = a(t) \cos(3\Omega t - \gamma) + \frac{\kappa}{(\omega^2 - \Omega^2)} \cos \Omega t + O(\varepsilon), \quad (12)$$

where the amplitude  $a$  and phase difference  $\gamma$  are determined by the differential equations

$$\frac{da}{dt} = \varepsilon \left( -\mu a - \frac{\alpha \Lambda^3}{\omega} \sin \gamma \right) \quad \text{and} \quad (13)$$

$$a \frac{d\gamma}{dt} = \varepsilon \left[ \left( \sigma - \frac{3\alpha \Lambda^2}{\omega} \right) a - \frac{3\alpha}{8\omega} a^3 - \frac{\alpha \Lambda^3}{\omega} \cos \gamma \right], \quad (14)$$

where  $\Lambda = \kappa(\omega^2 - \Omega^2)^{-1/2}$ . To determine the character of the solutions the singular points, found by setting  $(da/dt) = (d\gamma/dt) = 0$ , can be obtained:

$$\left[ \mu^2 + \left( \sigma - 3 \frac{\alpha \Lambda^2}{\omega} - \frac{3}{8} \frac{\alpha}{\omega} a^2 \right)^2 \right] a^2 = \frac{\alpha^2 \Lambda^6}{\omega^2}. \quad (15)$$

Equation (15) is an implicit equation for the amplitude of the response  $a$  as a function of the detuning parameter  $\sigma$  and the amplitude of the excitation  $\kappa$ . It can be seen that the peak amplitude  $a_p$  of the free-vibration term is given by  $\alpha \Lambda^3 / \mu \omega$ , which depends on  $\alpha$ . Thus, if  $\alpha = 0$ , then the amplitude of the free-vibration term decays to zero at steady state.

In the same way as before, the above analytical procedure can be extended to non-stationary responses.

### (3) Non-stationary Response of the Duffing Equation

Figure 8 shows the steady-state and non-stationary response curves for primary and secondary resonances for several rates of change,  $r$ . Here,  $r = 0$  corresponds to the quasi-steady response.

For the quasi-steady response, the actual solution is determined by the initial condition of the system, which affects the occurrence of the jump phenomena. When the detuning parameter  $\sigma$  is gradually increased, the amplitude increases smoothly. If  $\sigma$  is increased further, then a downward jump occurs. Furthermore, as  $\sigma$  is increased still further, the amplitude continues to decrease. In the reverse process, as  $\sigma$  is decreased, the amplitude gradually increases smoothly. If  $\sigma$  is increased further, then an upward jump occurs. Furthermore, as  $\sigma$  is decreased still further, the amplitude decreases. The jump phenomena are a result of the hysteresis caused by nonlinearity. On the other hand, there are no jump phenomena for a linear response and the same response is obtained whether  $\sigma$  is increased or decreased.

For a non-stationary response  $r \neq 0$ , the detuning parameter  $\sigma$  is increased or decreased around primary and secondary resonances. When  $\sigma$  increases, the peak amplitude of the response decreases, and the frequency where this peak occurs is increased as  $r$  increases. After passage through resonance, a beat phenomenon develops in the response and then decays. The peak amplitude can be found for smaller  $r$ . On the other hand, the same characteristic can be observed when  $\sigma$  decreases. Furthermore, the smaller  $\alpha$  becomes, the more symmetric the frequency-response curves for increasing  $\sigma$  and decreasing  $\sigma$  become. It can be seen that the nonlinear effects become apparent when the rate,  $r$ , of passage through resonance is small.

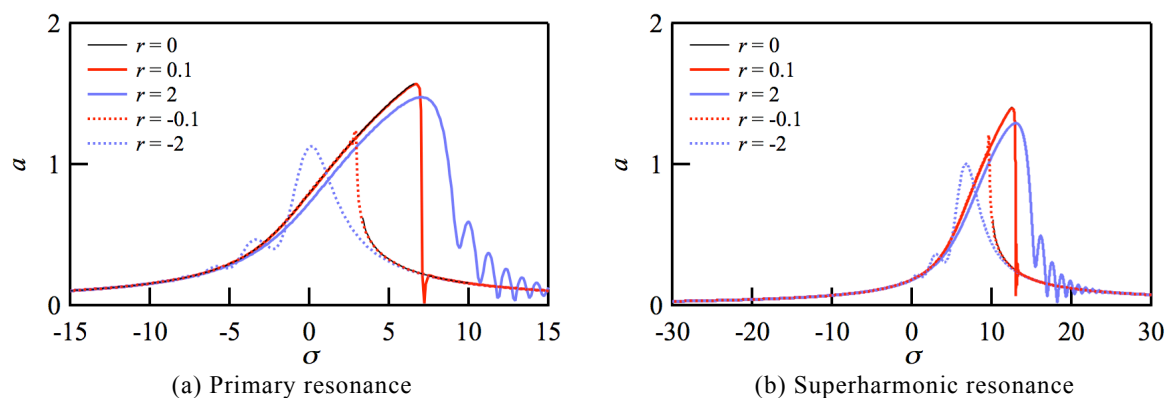


Figure 8 – Non-stationary frequency-response curves for primary and secondary resonances

## 4.2. Basic Concept for Nonlinear System Identification

Here we discuss the basic concept for the application of the time-frequency analysis to nonlinear system identification in order to model mechanical systems and determine system parameters (14, 15).

The easiest method to identify nonlinear parameters or systems is to examine the quasi-steady response of the system. However, it is quite difficult to conduct and verify the experiment under such conditions. This is because practical mechanical systems are continuously operated. Our aim is to establish a simple method of system identification without using any other measurements apart from output signals, measured during actual field operations. Therefore, we concentrate on passage through resonance at startup and shutdown while running. Thus, using the non-stationary response discussed in Section 3, there may be some possibility to model the system and to identify the parameters in Eq. (2).

If the system can be assumed to be modeled by the Duffing equation with weakly nonlinearity, then the system parameters are given by the non-stationary response, as shown in Figures 3 and 4. The system parameters for the primary resonance can be determined by the following procedure.

- (1) The rate,  $r$ , of increasing or decreasing the frequency of the excitation corresponds to the slope between the peak amplitude of excitation and the excitation frequency. It can be seen that when the free vibration is small, the scale of the color contour mapping in the time-frequency distribution result must be changed in order to recognize the free vibration.
- (2) The natural frequency  $\omega$  can be estimated by the free-damped vibration, which appears in the time-frequency analysis distribution. The free-damped vibration can be observed at the beginning of the vibration and after the passage through resonance.
- (3) When  $\mu$  is small, the value of  $\mu$  is determined by the decay of the free damped vibration, which appears in the time-frequency analysis distribution. These results were experimentally confirmed in (13).
- (4) The excitation force  $\kappa$  is determined by the peak amplitude  $a_p$ , that is,  $\kappa = 2\mu\omega a_p$ . It can be seen that if the rate,  $r$ , of increasing or decreasing the frequency of the excitation is relatively fast, then the peak amplitude at resonance is small compared to the stationary response of the system.
- (5) If the frequency response curves are symmetric about  $\sigma = 0$ , then the system has the properties of a linear spring. That is,  $\alpha = 0$ .
- (6) On the other hand, if the frequency response curves are not symmetric but differ from each other, then the system is nonlinear. That is,  $\alpha \neq 0$ . From the value of  $\sigma$  where the jump phenomena occurs,  $\alpha$  can be determined using Eq. (8).

We can thus obtain the nonlinear system parameters as shown in Figures 3 and 4 from the time-frequency analysis distributions. The remaining problems are parametric studies to determine which parameters will have an effect on the time-frequency analysis result. Using the same method, we can identify the parameters of the nonlinear system shown in Figures 6 and 7 from the time-frequency analysis distributions.

The advantage of the proposed modeling procedure lies in experimental studies. When we observe a nonlinear effect in the traditional way, several experiments must be conducted under the condition that the amplitude of the excitation is held fixed, which is not realistic in field conditions. Thus, the frequency of the excitation must be varied very slowly through the resonance, and the amplitude of the harmonic response observed carefully. Such a process will require more time than the time-frequency analysis.

In a practical mechanical system, not only the excitation frequency  $\Omega$  but also the amplitude of excitation  $\kappa$  may be varied when the system is started and shutdown while running. Therefore, further investigations must be made to identify the nonlinear systems. However, the identification procedure will be one of the basic concepts for actual field operations. With the use of the time-frequency analysis distributions we can model or identify other nonlinear systems, such as parametric excitation systems, in the same manner. Through this study, we could construct a database of various nonlinear systems. Such a database will allow us to model and identify nonlinear systems in real operational contexts.

## 5. CONCLUSIONS

The main purpose of this study was to model and identify the system parameters of structures and machines based on vibrational output signals. In this paper, we used our time-frequency analysis method to identify nonlinear vibrations. We discussed the time-frequency analysis of the Duffing equation, as a typical weakly nonlinear system. Thus, comparison between the time-frequency analysis result and the appropriate analytical solution was made at steady state. The time-frequency analysis of the Duffing equation for transient and non-stationary responses, represented by passage through resonance phenomena, was examined and the basic concept for the application of the time-frequency analysis to nonlinear system identification was discussed.

As a result, the effects of nonlinearity could be clarified. In particular, it was confirmed that the secondary resonance peculiar to nonlinear vibration for a non-stationary response can be explained with the method. Furthermore, comparison between the time-frequency analysis results and the appropriate analytical solution was made for both steady-state and slowly varying non-stationary responses. Finally, we discussed application of the time-frequency analysis to nonlinear system identification in order to model mechanical systems and determine system parameters.

Further investigation must be made to identify nonlinear systems. Throughout this study, we could construct a database of various nonlinear systems. Such a database will lead us to model and identify nonlinear systems in real operational contexts.

## ACKNOWLEDGEMENTS

This work was supported by JSPS KAKENHI Grant Number 25420197.

## REFERENCES

1. Yamamoto T, Ishida Y. Linear and nonlinear rotordynamics, John Wiley & sons, inc.; 2001.
2. Ed. Kuts M. Mechanical engineers' handbook, John Wiley & sons, inc.; 2005.
3. Cohen L. Time frequency analysis: Theory and applications, Prentice Hall; 1994.
4. Steve S, Liu M. Control of cutting vibration and machining instability: a time-frequency approach for precision, micro and nano machining, John Wiley & sons, inc.; 2013.
5. Burrus S, Gopinath R, Guo H. Introduction to wavelet and wavelet transform, Prentice Hall; 1997.
6. Kobayashi M, Aoyama S. Transient response analysis of a high speed rotor using constraint real mode synthesis, *Journal of Environment and Engineering*, 2011: 6 (3): 527-541.
7. Song Y, Sato H, Iwata Y, Komatsuzaki T. The response of a dynamic vibration absorber system with a parametrically excited pendulum, *Journal of Sound and Vibration*, 2003: 259 (4): 747-759.
8. Vermot G, Balmes E, Pasquet T, Lemaire R. Time/frequency analysis of contact-friction instabilities. application to automotive brake squeal, *Proceeding of international conference on noise and vibration engineering*, 2010: 4383-4398.
9. Yamazaki T, Ishikawa K, Stanislav M, Kuroda K. Study on transient statistical energy analysis by using two identical oscillator system, *Trans. JSME C*, 2008: 74 (740): 773-779 (in Japanese).
10. Yamazaki T, Stanislav M. An experimental method to verify impulsive responses on flat plate structure predicted by transient statistical energy analysis (TSEA), *Trans. JSME C*, 2011: 77 (776): 1201-1212 (in Japanese).
11. Ogata K. Discrete-time control system, Prentice-Hall; 1987.
12. Itoh Y, Yamaguchi N, Yamazaki T. Vibration analysis based on time-frequency analysis with digital filter, *Journal of system design and dynamics*, 2013: 7 (4): 441-455.
13. Itoh Y, Yamazaki T, Kato Y, Imazu T, Kudoh K, Takemura K. Modeling of vibration based on time-frequency analysis with digital filter, *Proceedings USB memory of JSME, Dynamics and design conference*, 2013: 317.pdf (in Japanese).
14. Imazu T, Yamazaki T, Itoh Y. Vibration transmission through bridge of violin, *Proceedings USB memory of JSME, Dynamics and design conference*, 2013: 361.pdf (in Japanese).
15. Imazu T, Yamazaki T, Itoh Y, Nakamura H. Impact Modeling between violin bridge and front plate in dynamic response analysis, *Proceedings CD memory of JSME*, 2014: 20902.pdf (in Japanese).
16. Nayfeh A, Mook D. Nonlinear oscillations, John Wiley & sons, inc.; 1979.